Geosci. Model Dev. Discuss., 8, 4075–4112, 2015
www.geosci-model-dev-discuss.net/8/4075/2015/
doi:10.5194/gmdd-8-4075-2015


Geoscientific Model Development Discussions
Open Access



# A fully coupled Atmosphere–Ocean Wave modeling system (WEW) for the Mediterranean Sea: interactions and sensitivity to the resolved scales and mechanisms

**P. Katsafados**[1], **A. Papadopoulos**[2], **G. Korres**[3], **and G. Varlas**[1,2]

[1]Department of Geography, Harokopion University of Athens, 70 El. Venizelou Str., Athens, 17671, Greece
[2]Institute of Marine Biological Resources and Inland Waters, Hellenic Centre for Marine Research, Anavyssos, Attiki, Greece
[3]Institute of Oceanography, Hellenic Centre for Marine Research, Anavyssos, Attiki, Greece

Received: 2 March 2015 – Accepted: 4 May 2015 – Published: 27 May 2015

Correspondence to: P. Katsafados (pkatsaf@hua.gr)

Published by Copernicus Publications on behalf of the European Geosciences Union.







## Abstract

It is commonly accepted that there is an urgent need for a better understanding of the factors that contribute to the air–sea interaction processes and their feedbacks. In this sense it is absolutely important to develop advanced numerical prediction systems that treat the atmosphere and the ocean as a unified system. The realistic description and understanding of the exchange processes near the ocean surface, requires the exact knowledge of the sea state and its evolution. This can be achieved by considering the sea surface and the atmosphere as a continuously cross talking dynamic system. Therefore, this study aims to present the effort towards developing a new, high-resolution, two-way fully coupled atmosphere–ocean wave model in order to support operational and research activities. A specific issue that it is emphasized here is the determination and parameterization of the air–sea momentum fluxes under conditions of extremely high and time-varying winds. Software considerations, data exchange as well as computational and scientific performance of the coupled system, so-called WEW, are also discussed throughout this study. In a case study of high-impact weather and sea state event, the wind–wave parameterization scheme reduces the resulted wind speed and the significant wave height as a response to the increased aerodynamic drag over rough sea surfaces. Overall, WEW offers a more realistic representation of the momentum exchanges in the ocean wind–wave system and includes the effects of the resolved wave spectrum on the drag coefficient and its feedback on the momentum flux.

## 1 Introduction

There is an urgent need for a better understanding of the factors that contribute to the air–sea interaction mechanisms, and for the development of corresponding advanced prediction systems that treat the atmosphere and the sea as a unified system. The lack of consistent skill in present forecasting systems may be partially attributed to





GMDD
8, 4075–4112, 2015



inadequate surface and boundary-layer formulations, and the lack of full coupling to a dynamic ocean (Chen et al., 2007). Sea waves play a key role in the exchange of momentum, heat and turbulent kinetic energy at the air–sea interface. Wind waves, while being generated by the wind, extract energy and momentum from the atmosphere and therefore the drag that is felt by the atmosphere over the oceans becomes sea-state dependent. Furthermore, ocean waves affect the mixing of heat and momentum in the upper ocean layers.

For a better description and understanding of the exchange processes near the ocean surface, an accurate forecast of the evolution of the sea state requires to considering the coupled sea surface and atmosphere as a continuously cross-talking system. Generally, it is by now clear that, at shorter and even more at longer scales, reliable results can be obtained by considering the fluid layer surrounding Earth as a single system. This means to simulate the atmosphere and the ocean as a single fully coupled system and to construct multi-model, multi-scale integrated systems (Liu et al., 2011).

The development of fully coupled simulation systems between atmosphere and ocean is the "state of the art" in the research evolution of numerical models. The complex mechanism of the exchange of momentum, mass, salt condensation nuclei, latent and sensible heat between atmosphere and ocean has been improved by developing the coupling systems. The large-scale perturbations in the general circulation of atmosphere and ocean, the temporal variability of dynamical air–sea interaction and its feedbacks have already been digested into climate coupling systems (Battisti, 1988; Philander et al., 1992; Soden and Held, 2006; Roberts and Battisti, 2011). During the last years, the importance of the coupling at regional scales is a challenging research topic (Hodur et al., 2002; Lionello et al., 2003). Because of the limited spatial and short time interaction scales between atmosphere and ocean, the direct and sufficient response between the coupled models is a substantial factor (Warner et al., 2010).

Coupled atmosphere–ocean wave systems generally exchange near surface wind velocity, from the atmosphere to the surface wave and exchanges friction velocity from





GMDD
8, 4075–4112, 2015



wave to the atmosphere. The modeling of the wave field allows the introduction of a sea surface roughness feedback on the momentum flux (Lionello et al., 2003). Primarily, the change of the intense of a storm or a cyclone due to the wave and the drag coefficient variability, under strong wind conditions is a critical field of study. More specifically, the hurricane-force winds increase the drag coefficient magnitude of the sea surface that leads to a decrease of the wind speed and a change to the wind direction. Generally, the feedbacks ultimately create non-linear interactions between different components and can make it difficult to access the full impact on each specific model (Warner et al., 2010).

At numerical experiments using an atmosphere-wave model under ten hurricanes in the western Atlantic Ocean during 1998–2003, the Charnock drag coefficient was used for approaching of sea surface friction at different wave evolution stages (Charnock, 1955; Moon et al., 2004). As a result, under hurricane force winds (above $33\,m\,s^{-1}$), it is observed a positive forcing by the decrease of the sea surface friction as derived from the breaking waves. For that reason, the cyclones that had been simulated by wind–wave coupled models were developed slower than those simulated by non-coupled models. Additionally, the maximum friction velocity and sea surface roughness were much larger than their counterparts in an uncoupled system, with the large sea surface roughness located in areas with small wave ages and wind speed of $25–33\,m\,s^{-1}$ (Liu et al., 2011). Also, maximum low-level wind speeds were typically estimated $2–3\,m\,s^{-1}$ less due to the feedback of ocean wave-induced stress. However, local differences in excess of $7–10\,m\,s^{-1}$ were found in some coupled model simulations (Doyle, 2002; Renault et al., 2012). In addition to these wind speed differences, significant wave height maxima were reduced by approximately 10 % in the coupled simulations due to the enhanced roughness associated with the young ocean waves.

Following the above mentioned evidence, a number of agencies and institutes worldwide based their recent operational activities onto coupling systems. United States Geological Survey (USGS) operates the Coupled Ocean – Atmosphere – Wave – Sediment Transport (COAWST) Modeling System, which is integrated by the Model Cou-





GMDD
8, 4075–4112, 2015



pling Toolkit to exchange data fields between the ocean model ROMS, the atmosphere model WRF, the wave model SWAN, and the sediment capabilities developed as part of the Community Sediment Transport Modeling Project (Warner et al., 2010). The European Centre for Medium-Range Weather Forecasts (ECMWF) coupling system consists of several components: an atmospheric general circulation model, an ocean wave model, a land surface model, an ocean general circulation model, a data assimilation system and ensemble forecasting systems, producing forecasts from days to weeks and months ahead (Bechtold et al., 2008). The Earth system model (CNRM-CM5) is running operationally in Meteo-France and it consists of several existing models designed independently and coupled through the OASIS software (Redler et al., 2010). It includes ARPEGE model for the atmosphere, NEMO model for the ocean circulation, GELATO for the sea-ice, SURFEX for land and the ocean-atmospheric fluxes and TRIP to simulate river routing and water discharge from rivers to the ocean (Voldoire et al., 2012).

In this line, this paper describes the strategy and current following procedures in developing and evaluating a new, advanced, fully coupled atmosphere–ocean wave model for supporting the research and the operational activities of the Hellenic Centre for Marine Research (HCMR). A specific issue it is emphasized here is the determination, parameterization and the sensitivity of the air–sea momentum fluxes in a case study of extremely high and time-varying winds.

## 2 Overview of modeling components of the coupled system

The coupled system consists of two components: the atmospheric and the ocean-wave models of the POSEIDON system. The atmospheric component is based on the Workstation Eta non-hydrostatic limited area model (Papadopoulos et al., 2002; Janjic, 2001; Nickovic et al., 2001; Mesinger et al., 1988). The ocean-wave component is based on the fourth generation OpenMP (OMP) version of the WAM model (Monbaliu et al., 2000; Korres et al., 2011) and the resulted name of the coupled system is WEW.





GMDD
8, 4075–4112, 2015



## 2.1 The atmospheric model

The atmospheric model is based on an advanced version of the SKIRON/Eta mesoscale meteorological model which is a modified version of the Eta/NCEP model (Kallos et al., 1997; Nickovic et al., 2001; Papadopoulos et al., 2002). This version became the core of the second generation POSEIDON weather forecasting system (Papadopoulos and Katsafados, 2009) and is fully parallelized to run efficiently on any parallel computer platform. It uses a two-dimensional scheme for partitioning grid-point space to Message Passing Interface (MPI) tasks. MPI is a protocol for the data exchange and synchronization between the executing tasks of a parallel job.

The Eta model is designed to use either the hydrostatic approximation or the non-hydrostatic correction in order to be able to resolve high resolution atmospheric processes. The Eta is formulated as a grid-point model and the partial differential equations are represented by finite-difference schemes. The ETA model "native" grid is awkward to work with because the variables are on semi-staggered (e.g., the grid for winds is not the same as the grid for mass points) and non rectangular (number of points in $x$ axis is not constant in respect to $y$ axis) grids. More specifically, in the horizontal, the model is defined over the semi-staggered $E$ grid, as it is shown in Fig. 1.

The Eta model is well-documented and detailed descriptions of its dynamics and physics components can be found in several studies (e.g., Mesinger et al., 1988; Janjic, 1994; Janjic et al., 2001, and references therein). The air–sea momentum fluxes are mainly parameterized in the surface layer scheme based on the well-established Monin–Obukhov similarity theory. It provides the lower boundary conditions for the 2.5 level turbulence model and introduces the viscous sublayer for a more realistic representation of the near surface fluxes. Different viscous sublayer approaches are applied over ground and over water surfaces in the model. For the specific application special care was taken in the calculations of the 10 m wind. The calculations of the surface parameters within this viscous sublayer have an obvious advantage that decreases the level of uncertainty in the wind, air temperature and humidity fields near the surface.





GMDD
8, 4075–4112, 2015



## 2.2 The ocean wave model

The wave forecasting system is based on WAM Cycle-4 code parallelized using OMP directives. In order to reduce unrealistic energy loss at boundary points in cases where the waves propagate parallel and near the coast we followed the technique of Monbaliu et al. (2000) where an alternative octant propagation coordinate system was introduced in the original WAM model code. For the octant advection scheme, eight propagation directions are defined instead of four in the classical quadrant scheme. Although in terms of computational workload, the octant scheme almost doubles the CPU time required by the upwind advection quadrant scheme, the scheme has clear advantages over other conventional schemes especially near the coasts (Cavaleri and Sclavo, 1998).

The grid of the wave model for the Mediterranean and Black Seas expands over the geographical area 8° W–42° E and 29–48° N as it is shown in Fig. 1 with a resolution of 1/20° × 1/20°. The bathymetric map has been constructed from ETOPO 2 data (National Geophysical Data Center, 2006. 2 min Gridded Global Relief Data (ETOPO2) v2. National Geophysical Data Center, NOAA) using bi-linear interpolation and some degree of smoothing. In shallow areas of the two basins local corrections were introduced based on nautical charts issued by the Hellenic Navy Hydrographic Service.

The Mediterranean and Black Seas wave model is a standalone model since it has no open boundary towards the Atlantic basin. This is justified in the sense that no significant swell from the Atlantic Ocean is expected to propagate into the Mediterranean basin through Gibraltar Straits. The Dardanelles and Bosporus Straits are also considered to be closed boundaries thus no wave energy is advected between Black Sea and Marmara Sea and between the Marmara Sea and the Aegean. The model uses 24 directional bins (15° directional resolution) and 30 frequency bins (ranging between 0.05 and 0.793 Hz) to represent the wave spectra distribution. The model runs in shallow water mode without depth or current refraction.





GMDD
8, 4075–4112, 2015



## 3 The theoretical background

In the offline coupled mode, the atmospheric model parameterizes the momentum exchange at the air–sea interface by applying a viscous sublayer scheme (Janjic, 1994) in which, the roughness $z$ over the sea surface is estimated by the formula:

$$z_0 = \frac{a_w \cdot u_*^2}{g} \tag{1}$$

assuming a constant Charnock coefficient $a_w = 0.018$, throughout the simulation. The wave model in turn, receives the near surface wind components without providing any feedback to the atmosphere. Therefore no interaction is taking place between the two models.

In parallel, the WAM model considers a wind input source function to the wave spectrum equation based on Janssen's (1989, 1991) quasi-linear theory where the transfer of momentum from the wind to the wave field depends simultaneously on the wind stress and the sea state itself. Hence, the WAM model includes a set of diagnostic equations for modeling the sea surface roughness feedback on the near surface atmospheric boundary layer (Janssen, 1989). The spatial and temporal variability of the Charnock coefficient is estimated at each WAM timestep by

$$a_w = \frac{0.01}{\sqrt{1 - \tau_w/\tau}} \tag{2}$$

In Eq. (2) $\tau_w$ is the wave induced stress given by

$$\tau_w = \rho_w g \int \frac{k}{\omega} \cdot S_{in} \cdot d\omega \, d\theta \tag{3}$$

The wave induced stress is mainly determined by the high frequency part of the wave spectrum consisting of the waves that have the largest growth rate due to the wind. In





GMDD
8, 4075–4112, 2015



Eq. (3) $\rho_w$ is the density of sea water, $g$ is the gravitational acceleration, $S_{in}$ represents the wind input term in the wave model, $\omega$ is the angular frequency, $\theta$ is the propagation direction and $k$ is the wavenumber. The total stress $\tau$ is estimated as

$$\tau = \rho_a \cdot C_D \cdot U_{ref}^2 \tag{4}$$

where $\rho_a$ is the density of air, $U_{ref}$ is the wind speed at a reference height and $C_D$ is the drag coefficient equals to

$$C_D = \left( \frac{\kappa}{\log(z_{ref}/z_0)} \right)^2 \tag{5}$$

with $k$ being the von Karman constant. Combining Eqs. (4) and (5) the total stress is given by

$$\tau = \left( \frac{\kappa \cdot U_{ref}}{\log(z_{ref}/z_0)} \right)^2 \tag{6}$$

The estimated sea surface roughness length is

$$z_0 = \frac{0.01 \cdot \tau}{\rho_a \cdot g \cdot \sqrt{1 - \tau_w/\tau}} \tag{7}$$

Finally, the computed friction velocity

$$u_* = \sqrt{\tau/\rho_a} \tag{8}$$

is applied in the wind input source function $S_{in}$.

Therefore, in the fully coupled mode, WAM can provide the atmospheric model with consistent values of Charnock, roughness and the friction velocity at each timestep.





GMDD
8, 4075–4112, 2015



In the current version of WEW, the atmospheric model applies the variable Charnock parameter $a_w$ in the Eq. (1) for the estimation of the sea surface roughness length. According to the Mellor–Yamada–Janjic (MYJ) surface layer parameterization scheme (Janjic, 1994), a viscous sublayer is assumed over the oceans and operates under three sea state regimes: (i) smooth and transitional, (ii) rough, and (iii) rough with spray, depending on the roughness Reynolds number and finally on the friction velocity which is a monotonic function of $R_r$ (Janjic, 1994)

$$R_r = \frac{z_0 u_*}{\nu} \tag{9}$$

where $\nu = 1.5 \times 10^{-5}\,\mathrm{m^2\,s^{-1}}$ is the kinematic viscosity of the air (Fig. 2). Then, the estimated friction velocity from WAM is applied for the determination of the sea state regimes, instead of the friction velocity that is computed by the atmospheric model. In particular, the changes of the regimes have been set to $u_{*r} = 0.3\,\mathrm{m\,s^{-1}}$ and $u_{*s} = 0.7\,\mathrm{m\,s^{-1}}$.

The friction velocity of the atmospheric model is then estimated by

$$u_* = \left[\left(\frac{K_{\mathrm{Msfc}}}{\Delta z_e}\right)(U_{\mathrm{LM}} - U_{Z_U})\right]^{1/2} \tag{10}$$

where $K_{\mathrm{Msfc}}$ is the Mellor–Yamada level 2 discrete momentum exchange coefficient, $\Delta z_e$ is the depth of the atmospheric layer that is extended between the lowest model level and the height of the "dynamical turbulence layer" at the bottom of the surface layer. The final term is the scalar difference between the wind velocity estimated at the lowest model level and the velocity at a height $z$ above the surface where the molecular diffusivities are still dominant (usually at the height of the viscous sublayer). The depth of the viscous sublayer for the momentum is estimated by

$$z_U = \zeta \nu \frac{M\left(\frac{z_0 u_*}{\nu}\right)^{1/4}}{u_*} \tag{11}$$





GMDD
8, 4075–4112, 2015



where $\zeta = 0.50$ and $M$ is depending on the sea state regime. For smooth regime, $M = 35$, and when the flow ceases to be smooth, $M = 10$. The atmospheric roughness obtained from the Eq. (1) and the friction velocity from the Eq. (10) are then implemented for the estimation of the near surface ($Z_{U10} = Z_U + 10$) wind components.

## 4 Software considerations of the coupled system

In the two-way coupled mode the Eta and WAM models utilize different domain projections, integration time step, grid geometry and cell size. Therefore, a major effort has been done in order to homogenize and handle the data exchange between the atmospheric and the ocean-wave components of the coupled system. These exchanges are built upon the MPI directives since it becomes a standard for developing parallel applications (Snir et al., 1998). Under the parallel environment of Multiple Program Multiple Data (MPMD), the two components are carried out as parallel tasks on different processors and they exchange information in a direct way (Fig. 3). Thus, the parallel execution of the system is totally handled by the mpirun/mpiexec commands and the two components are keeping their own executables. The communication between the two models is practically done through MPI_Send and MPI_Recv calls at every source time step of the ocean-wave model integration and the system runs flawlessly combining both MPICH and OMP environments. After the initial development, the modification of each component source code is quite simple, just adding some data exchange routines and insert the appropriate commands in the original model code which call the coupling routines, and each component keeps its original structure.

At the initialization stage, the atmospheric model starts at first and loads the inter- and intra-communicators. The atmospheric model sends to the wave model the near surface wind components and receives the variable Charnock coefficient array, which is then used for the estimation of $z_0$ in the surface layer parameterization scheme. Each data exchange requires re-projection from the atmospheric model Arakawa-E grid to the ocean-wave model regular lat-lon grid and vice versa (Fig. 4). For consis-





GMDD
8, 4075–4112, 2015



tency, the sea-masks are exchanged at the initialization stage and the atmospheric to ocean-wave timesteps ratio is currently set to 1/24 but it can be adjusted to any other configuration through the main namelist of the system. Moreover, data exchanges can be easily expanded or cut off and the ocean-wave outputs (significant wave height and period, Charnock coefficient, friction velocity etc.) are finally redirected through the internal communicators as outputs of the atmospheric component.

The initial version (0) of WEW was configured on a $2 \times 2$ topology (2 additional processes are allocated for setting the I/O servers) for the atmospheric component (Fig. 5). The ocean-wave component is parallelized using OMP directives and it was configured with 2 threads. The current version Eq. (5) has been configured on a very fine horizontal resolution of $1/20^{\circ} \times 1/20^{\circ}$ with $493 \times 461$ E-grid points and $1001 \times 381$ regular lat-lon points. Numerous tests have been performed in order to extract the optimum topology. To this end, 28 threads have been allocated in total, 20 are dedicated to the execution of atmospheric component and the rest 8 are reserved to the ocean-wave component. Thus, WEW is running on a Dual Quad cores Intel Xeon platform cluster using in total 28 threads at 4 nodes but it is easily portable in any other architecture and flexible to adopt a different topology. For the abovementioned configuration WEW requires almost 10 min for each simulation hour.

A multi-level flowchart of the system and the data exchanges are depicted in Fig. 6. In the offline coupling mode (CTRL hereafter) the atmospheric component sends hourly near surface wind velocity to the ocean-wave model without any other interaction between the two models (red line). In the two-way fully coupled mode (WEW hereafter) the atmospheric model sends at every WAM model timestep the near surface wind components and receives various near sea surface variables. In more details, WAM for each timestep can provide to atmospheric model with consistent values of Charnock coefficient, friction velocity, total surface stress etc. In the current version, the atmospheric model ingests Charnock coefficient and friction velocity values into the Mellor Yamada surface layer parameterization scheme for the next timestep estimation of the





GMDD
8, 4075–4112, 2015



near surface wind components and the accurate determination of the viscous sublayer and the parameterization of the air–sea momentum fluxes.

## 5 System configuration

The consistency and performance of WEW has been extensively evaluated through various simulations for preselected case studies. The domain of integration encompasses the Mediterranean Sea and the Black Sea on a horizontal resolution of $0.05^\circ \times 0.05^\circ$ (Fig. 7). However, various tests of the system at the initial stages of the development performed on the coarser grid of $0.10^\circ \times 0.10^\circ$. Gridded data from the European Centre for Medium range Weather Forecast (ECMWF) were used as initial and boundary conditions of the atmospheric component. The grid of the wave model for the Mediterranean and Black Seas covers the geographical area 8° W–42° E and 29–48° N as it is shown in Fig. 7 (black line) on a similar to the atmospheric component resolution. The different projection of the two components yields a mismatch between the two domains. Thus, a constant Charnock coefficient $a_w = 0.018$ was implemented for the sea grid points of the atmospheric domain (near its western boundary) which were outside the WAM model domain. A 1-2-1 smoothing filter is also applied over the transition zone of the ocean-wave domain to the atmospheric one in order to reduce artificial generated waves. The initialization of WAM was based on a wind–sea spectrum computed on the basis of the initial wind field and it was produced in the preprocessing stage of the atmospheric model (cold start).

Each component of WEW kept its own timestep. The propagation timestep of the WAM model was 120 s while its source timestep was 360 s. The coupling procedure exchanges data on the source timestep of WAM model, $DT_w = 360$ s. As the timestep of the atmospheric model was $DT_a = 15$ s the exchanging procedure activated every 24 timesteps of the atmospheric model. Every hour WEW stored its unified outputs (including atmospheric and ocean-wave fields) on the native Arakawa-E grid. The configuration of the system is summarized in the Table 1.





GMDD
8, 4075–4112, 2015



## 6 Application and performance of the WEW system

WEW has been tested for its consistency and performance in a high-impact atmospheric and sea state case study of an explosive cyclogenesis in Ligurian Sea. The performance of the fully two-way coupled system (WEW) was statistically evaluated over sea areas against its performance in the offline coupling mode (CTRL). The evaluation was based on the point-to-point comparison with remote sensed and in situ observations for the case using as reference the network of 39 available buoys in the Mediterranean Sea (Fig. 8). The system was also evaluated against remote sensed data retrieved from CRYOSAT, ENVISAT, ESR2 and JASON1/2.

The incident of 4–11 January 2012, has been selected due to the severity of the prevailed atmospheric conditions characterized by an explosive cyclogenesis in Ligurian Sea (Varlas et al., 2014). In more details, on 5 January 2012 a low pressure system was formed over the cyclogenetic area of the Ligurian Sea. It was mainly triggered by a widespread upper-level trough extended from the Central Europe to the Mediterranean Sea (Fig. 9a). The upper-level trough rapidly intensified the system and supported its southeastern movement (Fig. 9b). On 6 January the system was moved towards the Eastern Mediterranean, where the pressure dropped more than $24\sin\varphi/\sin 60^{\circ}$ hPa in 24 h, defining the event as explosive cyclogenesis event (Fig. 10 a and b). During 6 and 7 January, the strong pressure gradient provoked gale force winds and significant storm surge over a vast area including Central Mediterranean and the Aegean Sea. It is noteworthy that the buoys at the Ligurian and Balearic Seas recorded wind speeds exceeding 20 $\mathrm{m\,s^{-1}}$ and significant wave height over 5 m.

The horizontal distributions of the wind speed and the SWH as well as their differences between WEW and CTRL experiment are depicted in Fig. 11. On 6 January 2012 at 18:00 UTC, winds exceeding the 22 $\mathrm{m\,s^{-1}}$ and SWH over 8 m cover a large part of the Mediterranean Sea (Fig. 11 a and b). The horizontal distribution of differences between WEW and CTRL experiments reveal a systematic reduction of the wind speed and the SWH in the two-way fully coupled mode (WEW). The near surface wind speed





GMDD
8, 4075–4112, 2015



differences are varied up to 2 m s$^{-1}$ and they are located over the areas where maximum wind velocities occurred (Fig. 11c). The reduced wind speed simulated by WEW, as a feedback of the enhanced sea surface roughness, impacts the estimated SWH as well (Fig. 11d). Thus, SWH differences up to 1.2 m are located over the areas of the maximum wind speed reduction (e.g. the area between the Balearic and Tyrrhenian Seas). Similar results have been also drawn by Doyle (2002), Liu et al. (2011) and Renault et al. (2012).

The outputs from both simulations, CTRL and WEW, have been statistically evaluated based on the point-to-point hourly comparison between model-generated variables and the available Mediterranean buoys measurements. Hourly pairs of observed and estimated values were obtained using the nearest-neighbor interpolation technique, taking care of whether this nearest source point is sea masked grid point. Both simulations slightly underestimate the near surface wind speed exceeding 1 m s$^{-1}$. The underestimation is more prominent for the wind speeds exceed the 8 m s$^{-1}$ (Fig. 12a). Although WEW increase the underestimation, it offers an overall improvement of the RMS error by approximately 2 %. Additionally, it decreases the standard deviation (STD Mod) towards the STD of the buoys. In accordance with the wind speed, the bias scores of the significant wave height (SWH) indicate an underestimation for the CTRL simulation more prominent in WEW (Fig. 12b). However, WEW offers an overall improvement more than 7 % of the SWH error, with 0.53 instead of 0.57 m s$^{-1}$, and increased correlation coefficients.

The systematic underestimation of the wind speed persists in the evaluation against the remote sensed data referenced in this section. The WEW enhances the underestimation of CTRL but it also reduces the RMSE by 1.5 % (Fig. 12c). In contrast to the slight overestimation of the CTRL, WEW underestimates the SWH as well (Fig. 12d). It further improves the entire statistical scores and shows a RMSE decrease by almost 11 %. Entire indexes are also statistically significant in 95 % confidence level. This is attributed to the fact that the application of the two-way fully coupled system can overall generate and support a more realistic near sea surface circulation pattern by fully





GMDD
8, 4075–4112, 2015



resolving air–sea interaction processes at the relevant interface, including wind speed regime and wave patterns.

### 6.1 Physical interpretation

The particular interactions considered in WEW are mainly driven by the momentum exchanges in the ocean wind–wave system. The fully coupled wind–wave parameterization scheme includes effects of the resolved wave spectrum on the drag coefficient and its feedback on the momentum flux. In general, the feedbacks create non-linear interactions in the dynamic structure of a storm or a cyclone due to the time-space sea surface friction variability. In WEW simulations, the maximum friction velocity and sea surface roughness are much larger than their counterparts in CTRL, with the maxima located in areas with small wave ages and wind speed above $20\,m\,s^{-1}$. The increased near sea surface friction builds a more turbulent and deeper PBL preventing a faster evolution of the storm (Fig. 13).

The reduction of the near surface wind speed, as it was evidenced in WEW simulation and depicted in Fig. 11c, is mainly attributed to the variable Charnock coefficient directly ingested in the Eq. (1) for the roughness length estimation in the MYJ surface layer parameterization scheme. In CTRL and WEW experiments the Charnock coefficient logarithmically increases with the wind speed at about the $22\,m\,s^{-1}$ (Fig. 14). The enhanced Charnock coefficient increases the roughness length and decreases the near surface wind speed in WEW simulations. This is also affects the estimation of the significant wave height in the two-way coupled simulations. Especially in WEW, the saturation of the Charnock coefficient for wind speeds exceeding the $22\,m\,s^{-1}$ indicates that in extremely high wind conditions the sea surface friction conserves or decreases offering a positive forcing to the flow. Beyond this speed the sea surface does not become any rougher in aerodynamic sense. The saturation of the aerodynamic roughness, finally, leads to a flow separation due to the continuous wave breaking in areas where the flow is unable to follow the wave crests and troughs (Donelan et al., 2004). This wind–wave parameterization feature offers a more realistic representation of the





GMDD
8, 4075–4112, 2015



aerodynamic drag over rough sea surfaces. Similar findings have been also confirmed by relevant studies (eg. Bao et al., 2000; Makin, 2005; Chen et al., 2007).

The roughness length as a function of the friction velocity is characterized by an initial decrease as the surface condition goes from aerodynamically smooth to aerodynamically rougher regime (Fig. 15). This is the result of an aerodynamically smooth surface where the molecular motions are dominant in the developed viscous sublayer (Csanady, 2001). In moderate and fully rough sea state regimes the roughness length is exponentially increasing with the friction velocity. The roughness length in WEW experiment is substantially larger than in CTRL for friction velocities exceeding the $0.60\,m\,s^{-1}$. It also shows a tendency to saturation for friction velocities exceed the $1\,m\,s^{-1}$. This is an indication of the enhanced friction in WEW under rough sea state regimes as a result of the variable Charnock parameter in the surface layer parameterization scheme.

## 7 Concluding remarks and future perspectives

WEW is the recently developed two-way fully coupled atmosphere–ocean wave system for supporting air–sea interaction research and operational activities at HCMR. The system is built in the MPMD environment handling the atmospheric and the ocean-wave components as parallel tasks on different processors. In offline coupled mode, the atmospheric component parameterizes the air–sea momentum estimating the roughness length over the sea surface as a function of the constant Charnock coefficient throughout the simulation. The ocean-wave component passively receives the near surface wind components and there is no interaction between the two models. In WEW, the atmospheric model sends to the wave model the near surface wind components on its timestep frequency and receives the space–time variable Charnock field, which is directly applied in the surface layer parameterization scheme for the estimation of the roughness length.

Interactions considered in WEW are mainly driven by the momentum exchanges in the ocean wind–wave system and include the effects of the resolved wave spectrum





GMDD
8, 4075–4112, 2015



on the drag coefficient and its feedback on the momentum flux. As a general outcome, the maximum friction velocity and sea surface roughness are much larger than their counterparts in the offline coupling mode and this is resulted in a more turbulent and deeper marine PBL. The reduction of the near surface wind speed in the fully coupled simulation is mainly attributed to the enhanced Charnock coefficient which increases the roughness length and finally decreases the significant wave height. The Charnock coefficient logarithmically increases with the wind speed at about the $22\,m\,s^{-1}$ and the saturation above indicates that in extremely high wind conditions the sea surface friction conserves or decreases offering a positive forcing to the flow. This wind–wave parameterization feature offers a more realistic representation of the aerodynamic drag over rough sea surfaces (Chen et al., 2007).

The abovementioned responses have been also tested in a high-impact atmospheric and sea state case study of an explosive cyclogenesis in the Mediterranean Sea. Despite the fact of the increased underestimation, affecting both wind speed and significant wave height, WEW offers an overall improvement of their RMS error up to 11 %. The underestimation is attributed to the direct implementation of the variable Charnock coefficient into the current surface layer parameterization scheme and it is more prominent to the gale force wind speeds. Therefore, an extended modification of the current MYJ scheme is required, and it is in near future authors' plans, in order to adjust it to the updated sea surface forcings dynamically obtained from the ocean-wave component. To this end, an alternative parameterization scheme is under development for the more realistic representation of the sea surface momentum exchange and its feedbacks in WEW.

## Code availability

For ETA model and WAM model users, the relevant code modifications for coupling the two numerical systems can be made available by Petros Katsafados (pkat-





GMDD
8, 4075–4112, 2015



saf@hua.gr), Anastasios Papadopoulos (tpapa@hcmr.gr) and Gerasimos Korres (gkorres@hcmr.gr).

**The Supplement related to this article is available online at doi:10.5194/gmdd-8-4075-2015-supplement.**

*Acknowledgements.* This research is supported by the EU funded project MyWave (FP7-SPACE-2011-1/CP-FP, SPA.2011.1.5-03). ISPRA and IFREMER (Globwave project) are gratefully acknowledged for the provision of buoy and satellite data respectively. ECMWF is also acknowledged for the kindly provision of the gridded analyses data.

## References

Bao, J. W., Wilczak, J. M., Choi, J. K., and Kantha, L. H.: Numerical simulations of air–sea interaction under high wind conditions using a coupled model: a study of hurricane development, Mon. Weather Rev., 128, 2190–2210, 2000.

Battisti, D. S.: Dynamics and thermodynamics of a warming event in a coupled tropical atmosphere–ocean model, J. Atmos. Sci., 45, 2889–2919, 1988.

Bechtold, P., Köhler, M., Jung, T., Doblas-Reyes, D., Leutbecher, M., Rodwell, M., Vitart, F., and Balsamo, G.: Advances in simulating atmospheric variability with the ECMWF model: from synoptic to decadal time-scales, Q. J. Roy. Meteor. Soc., 134, 1337–1351, 2008.

Cavaleri, L. and Sclavo, M.: Characteristics of quadrant and octant advection schemes in wave models, Coast. Eng., 34, 221–242, 1998.

Charnock, H.: Wind stress on a water surface, Q. J. Roy. Meteor. Soc., 81, 639–640, 1955.

Chen, S. S., Zhao, W., Donelan, M. A., Price, J. F., and Walsh, E. J.: The CBLAST-Hurricane program and the next-generation fully coupled atmosphere–wave–ocean models for hurricane research and prediction, B. Am. Meteorol. Soc., 88, 311–317, 2007.

Csanady, G. T.: Air–Sea Interaction: Laws and Mechanisms, Cambridge University Press, ISBN 0521796806, 25–26, 2001.





GMDD
8, 4075–4112, 2015



Donelan, M. A., Haus, B. K., Reul, N., Plant, W. J., Stiassnie, M., Graber, H. C., Brown, O. B., and Saltzman, E. S.: On the limiting aerodynamic roughness of the ocean in very strong winds, Geophys. Res. Lett., 31, 4539–4542, 2004.

Doyle, J. D.: Coupled atmosphere–ocean wave simulations under high wind conditions, Mon. Weather Rev., 130, 3087–3099, 2002.

Hodur, R. M., Pullen, J., Cummings, J., Hong, X., Doyle, J. D., Martin, P., and Rennick, M. A.: The Coupled Ocean/Atmosphere Mesoscale Prediction System (COAMPS), Oceanography, 15, 88–98, 2002.

Janjić, Z. I.: The step-mountain eta coordinate model: further developments of the convection, viscous sublayer, and turbulence closure schemes, Mon. Weather Rev., 122, 927–945, 1994.

Janjic, Z. I., Gerrity Jr., J. P., and Nickovic, S.: An alternative approach to nonhydrostatic modeling, Mon. Weather Rev., 129, 1164–1178, 2001.

Janssen, P. A. E. M.: Wave-induced stress and the drag of air flow over sea waves, J. Phys. Oceanogr., 19, 745–754, 1989.

Janssen, P. A. E. M.: Quasi-linear theory of wind-wave generation applied to wave forecasting, J. Phys. Oceanogr., 21, 1631–1642, 1991.

Kallos, G., Nickovic, S., Papadopoulos, A., Jovic, D., Kakaliagou, O., Misirlis, N., Boukas, L., Mimikou, N., Sakellaridis, G., Papageorgiou, J., Anadranistakis, E., and Manousakis, M.: The regional weather forecasting system SKIRON: an overview, in: Proceedings of the Symposium on Regional Weather Prediction on Parallel Computer Environments, Athens, Greece, 15–17 October 1997, 109–122, 1997.

Korres, G., Papadopoulos, A., Katsafados, P., Ballas, D., Perivoliotis, L., and Nittis, K.: A 2 year intercomparison of the WAM-Cycle4 and the WAVEWATCH-III wave models implemented within the Mediterranean Sea, Medit. Mar. Sci., 12, 129–152, 2011.

Lionello, P., Martucci, G., Zampieri, M.: Implementation of a coupled atmosphere–wave–ocean model in the Mediterranean Sea: sensitivity of the short time scale evolution to the air–sea coupling mechanisms, Glob. Atmos. Ocean Syst., 9, 65–95, 2003.

Liu, B., Liu, H., Xie, L., Guan, C., and Zhao, D.: A coupled atmosphere–wave–ocean modeling system: simulation of the intensity of an idealized tropical cyclone, Mon. Weather Rev., 139, 132–152, 2011.

Makin, V. K.: A note on the drag of the sea surface at hurricane winds, Bound-Lay. Meteorol., 115, 169–176, 2005.





GMDD
8, 4075–4112, 2015



Mesinger, F., Janjic, Z. I., Nickovic, S., Gavrilov, D., and Deaven, D. G.: The step-mountain coordinate: model description and performance for cases of Alpine lee cyclogenesis and for a case of an Appalachian redevelopment, Mon. Weather Rev., 116, 1493–1518, 1988.

Monbaliu, J., Hargreaves, R., Albiach, J., Luo, W., Sclavo, M., and Günther, H.: The spectral wave model, WAM, adapted for applications with high spatial resolution, Coast. Eng., 41, 41–62, 2000.

Moon, I., Ginis, I., and Hara, T.: Effect of surface waves on Charnock coefficient under tropical cyclones, Geophys. Res. Lett., 31, L20302, doi:10.1175/1520-0469(2004)061<2334:EOSWOA>2.0.CO;2, 2004.

Nickovic, S., Kallos, G., Papadopoulos, A., and Kakaliagou, O.: A model for prediction of desert dust cycle in the atmosphere, J. Geophys. Res., 106, 18113–18129, 2001.

Papadopoulos, A. and Katsafados, P.: Verification of operational weather forecasts from the POSEIDON system across the Eastern Mediterranean, Nat. Hazards Earth Syst. Sci., 9, 1299–1306, doi:10.5194/nhess-9-1299-2009, 2009.

Papadopoulos, A., Katsafados, P., Kallos, G., and Nickovic, S.: The weather forecasting system for POSEIDON – An overview, Glob. Atmos. Ocean Syst., 8, 219–237, 2002.

Philander, S. G. H., Pacanowski, R. C., Lau, N. C., and Nath, M. J.: Simulation of ENSO with a global atmospheric GCM coupled to a high-resolution, tropical Pacific Ocean GCM, J. Climate, 5, 308–329, 1992.

Redler, R., Valcke, S., and Ritzdorf, H.: OASIS4 – a coupling software for next generation earth system modelling, Geosci. Model Dev., 3, 87–104, doi:10.5194/gmd-3-87-2010, 2010.

Renault, L., Chiggiato, J., Warner, J. C., Gomez, M., Vizoso, G., and Tintoré, J.: Coupled atmosphereoceanwave simulations of a storm event over the Gulf of Lion and Balearic Sea, J. Geophys. Res., 117, C09019, doi:10.1029/2012JC007924, 2012.

Roberts, W. H. and Battisti, D. S.: A new tool for evaluating the physics of coupled atmosphere–ocean variability in nature and in general circulation models, Clim. Dynam., 36, 907–923, 2011.

Soden, B. J. and Held, I. M.: An assessment of climate feedbacks in coupled ocean–atmosphere models, J. Climate, 19, 3354–3360, 2006.

Snir, M., Otto, S., Huss-Lederman, S., Walker, D., and Dongarra, J.: MPI – The Complete Reference, Massachusetts Institute of Technology, ISBN 0-262-69215-5, 1998.

Varlas, G., Papadopoulos, A., Korres, G., and Katsafados, P.: Modeling the air–sea wave interaction processes in an explosive cyclone over the Mediterranean Sea, in: 12th International





GMDD
8, 4075–4112, 2015



Conference on Meteorology, Climatology and Atmospheric Physics (COMECAP 2014), University of Crete, Heraklion, Crete, Greece, 28–31 May 2014, 3, 289–294, 2014.

Voldoire, A., Sanchez-Gomez, E., Salas y Mélia, D., Decharme, B., Cassou, C., Sénési, S., Valcke, S., Beau, I., Alias, A., Chevallier, M., Déqué, M., Deshayes, J., Douville, E., Fernandez, G., Madec, E., Maisonnave, M.-P., Moine, S., Planton, D., Saint-Martin, H., Szopa, S., Tyteca, S., Alkama, R., Belamari, S., Braun, A., Coquart, L., and Chauvin, F.: The CNRM-CM5.1 global climate model: description and basic evaluation, Clim. Dynam., 40, 2091–2121, 2012.

Warner, J. C., Armstrong, B., He, R., and Zambon, J. B.: Development of a coupled ocean–atmospher *e* wave–sediment transport (COAWST) modeling system, Ocean Model., 35, 230–244, 2010.





GMDD

8, 4075–4112, 2015



**Table 1.** The configuration of the WEW.

| WEW version 5 | Atmospheric component | Ocean wave component |
|---|---|---|
| Integration domain | Mediterranean Sea, Europe, Black Sea | |
| Grid | Arakawa semistaggered *E* grid defined in transformed lat/lon coordinate system | Regular lat/lon coordinate system |
| Horizontal grid increment | $0.05^{\circ} \times 0.05^{\circ}$ | |
| Vertical coordinate | Step mountain, $\eta$ coordinate | – |
| Vertical levels | 38 | – |
| Timesteps (s) | 15 | 120/360 |
| Initial and boundary conditions | ECMWF, $0.5 \times 0.5$, 11 isobaric levels, 6 h update of the boundary conditions | Initialization from the atmospheric component, refresh rate every 360 s |
| MPI/OMP topology | 16 MPI processing threads + 4 I/O servers = 20 | 8 OMP threads |





GMDD
8, 4075–4112, 2015



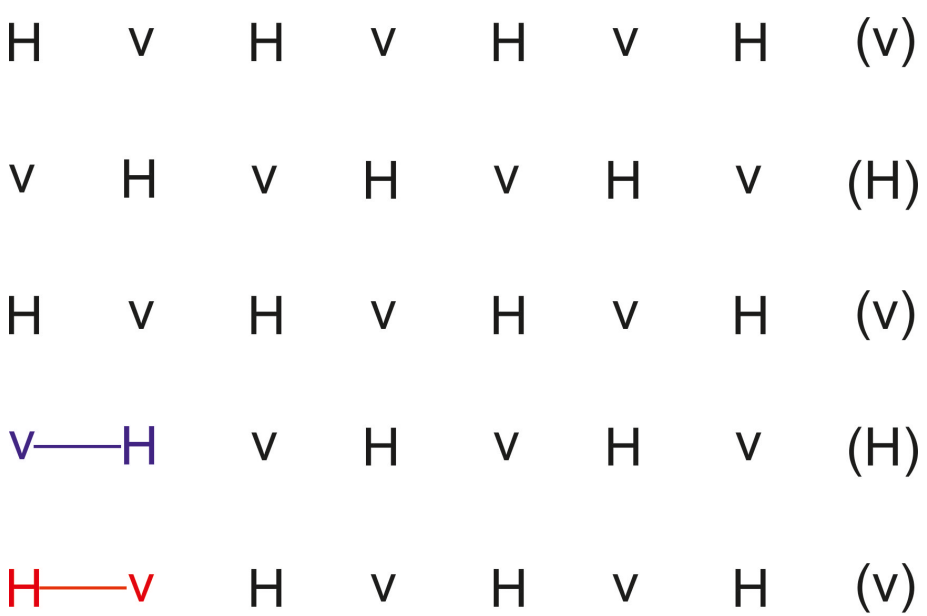


**Figure 1.** The E-grid stagger. The mass points represent by *H* and the wind points represent by *v*.





GMDD
8, 4075–4112, 2015



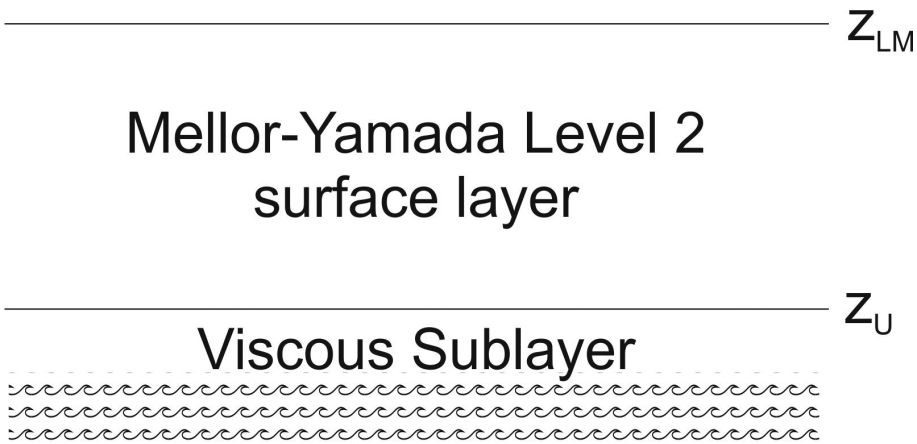


**Figure 2.** The Mellor–Yamada surface layer with the viscous sublayer over the ocean. The symbol $Z_{LM}$ is the height of the lowest model layer and $Z_U$ is the depth of the viscous sublayer for momentum (Reproduced from Janjic, 1994).





GMDD
8, 4075–4112, 2015





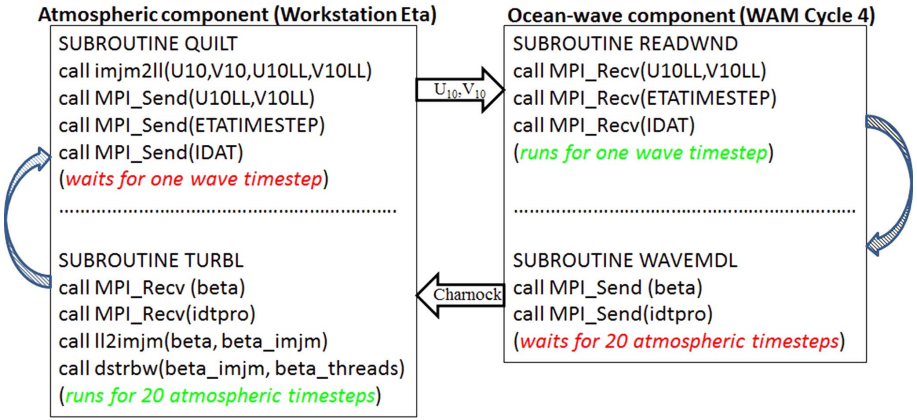


**Figure 3.** The WEW exchanges near surface $U, V$ components and Charnock coefficient every timestep of the ocean-wave model.





GMDD
8, 4075–4112, 2015



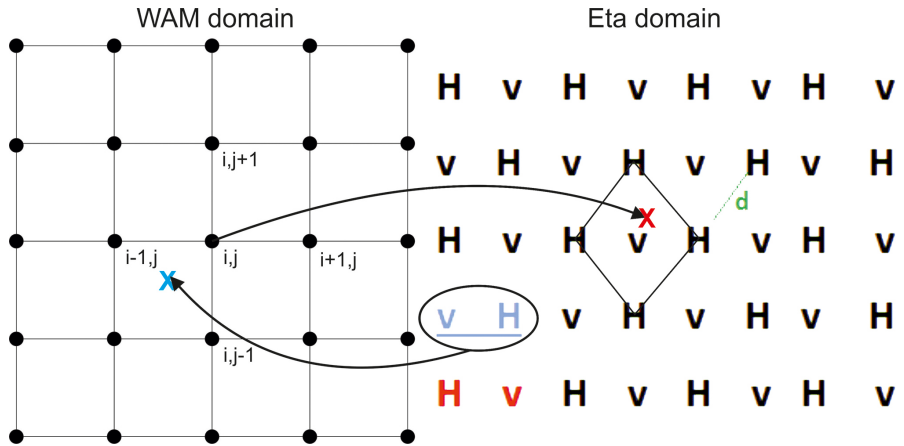


**Figure 4.** Sketch of the WEW multi-grid structure. The transformations from the Arakawa-E grid to the regular lat-lon grid and vice versa are also depicted.





GMDD
8, 4075–4112, 2015



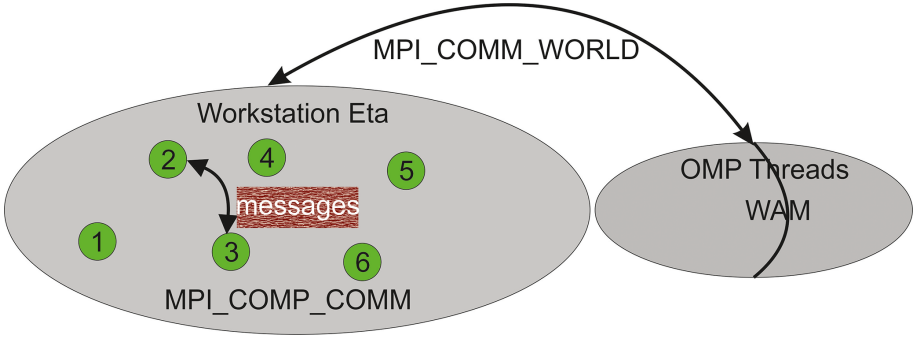


**Figure 5.** The WEW intra- and inter-communicators.





GMDD
8, 4075–4112, 2015



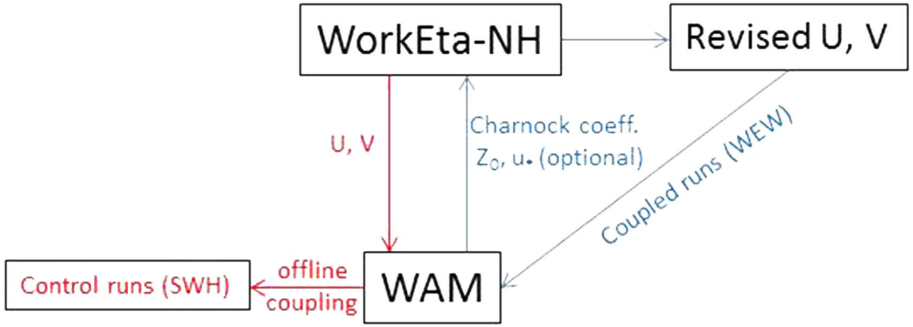


**Figure 6.** Informational flowchart for the offline coupled (red lines) and the two-way coupled simulations (blue lines).





GMDD
8, 4075–4112, 2015





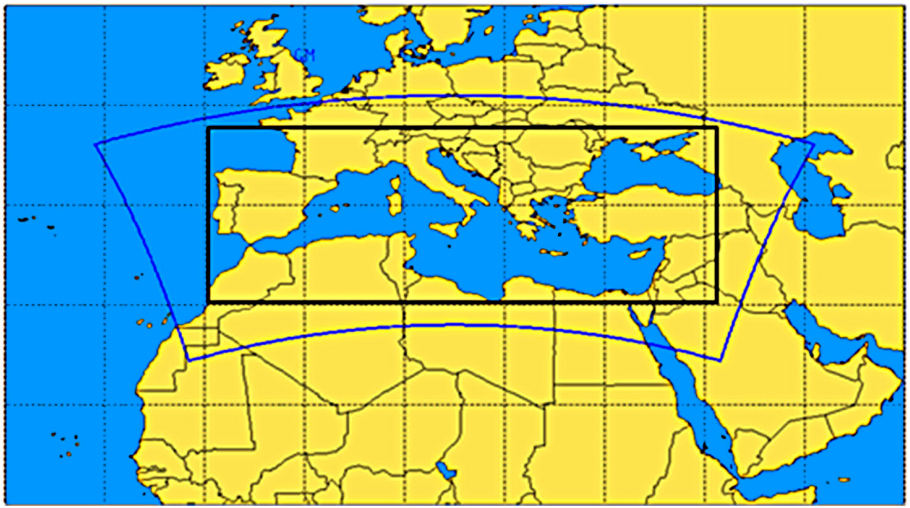

**Figure 7.** Current domains configuration of the atmospheric (blue line) and the ocean-wave models (black line).





GMDD
8, 4075–4112, 2015



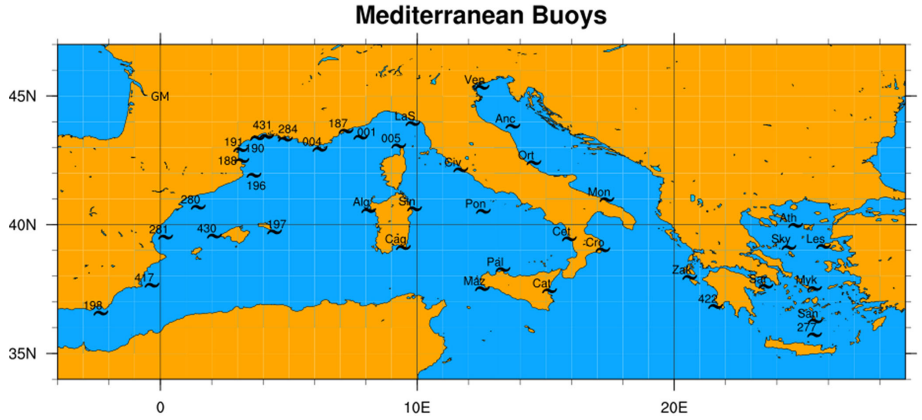


**Figure 8.** Spatial distribution of the Mediterranean buoys applied for the evaluation of the system. Data were made available from ISPRA in the framework of MyWave project.





GMDD
8, 4075–4112, 2015



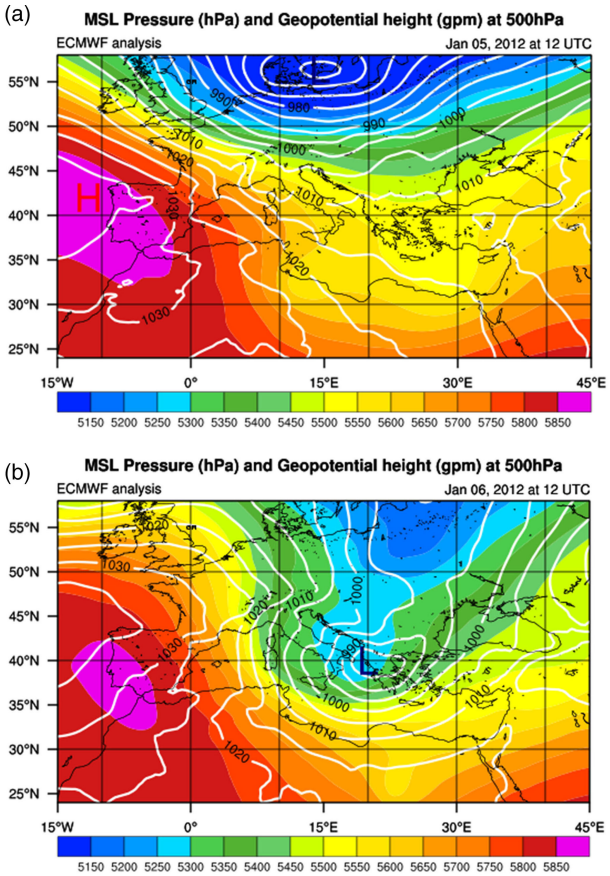


**Figure 9.** Mean Sea Level Pressure (contours in hPa) and geopotential height at 500 hPa (colored shaded in gpm) for **(a)** 5 January at 12:00 UTC **(b)** 6 January at 12:00 UTC, 2012. Data are based on ECMWF operational analysis.





GMDD
8, 4075–4112, 2015





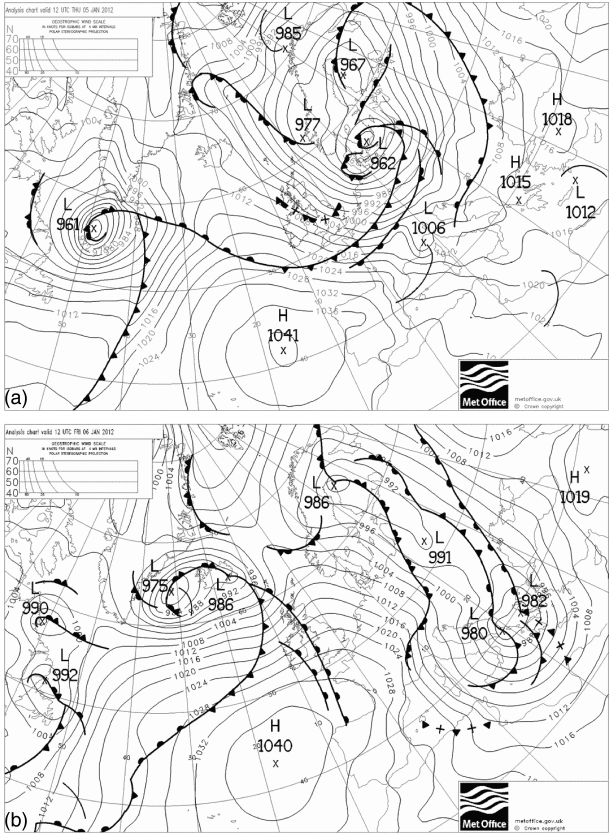


**Figure 10.** Surface pressure analysis map (mb) for **(a)** 5 January at 12:00 UTC **(b)** 6 January at 12:00 UTC, 2012. The maps derived from UK Met office surface analysis archive.





GMDD
8, 4075–4112, 2015





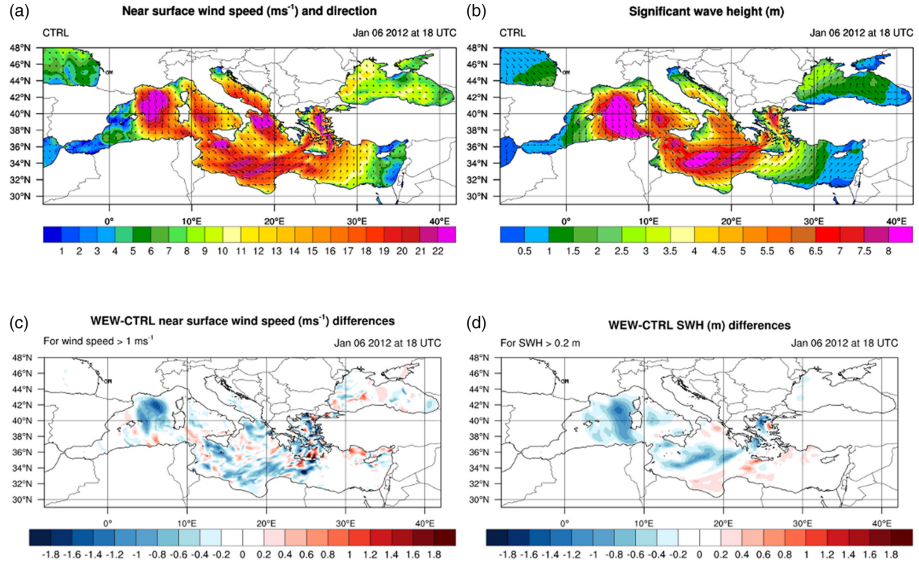


**Figure 11.** Panel of the horizontal distribution for the **(a)** wind speed, **(b)** SWH and their differences between WEW and CTRL experiments for the **(c)** wind speed and **(d)** SWH for 6 January 2012 at 18:00 UTC.





GMDD
8, 4075–4112, 2015





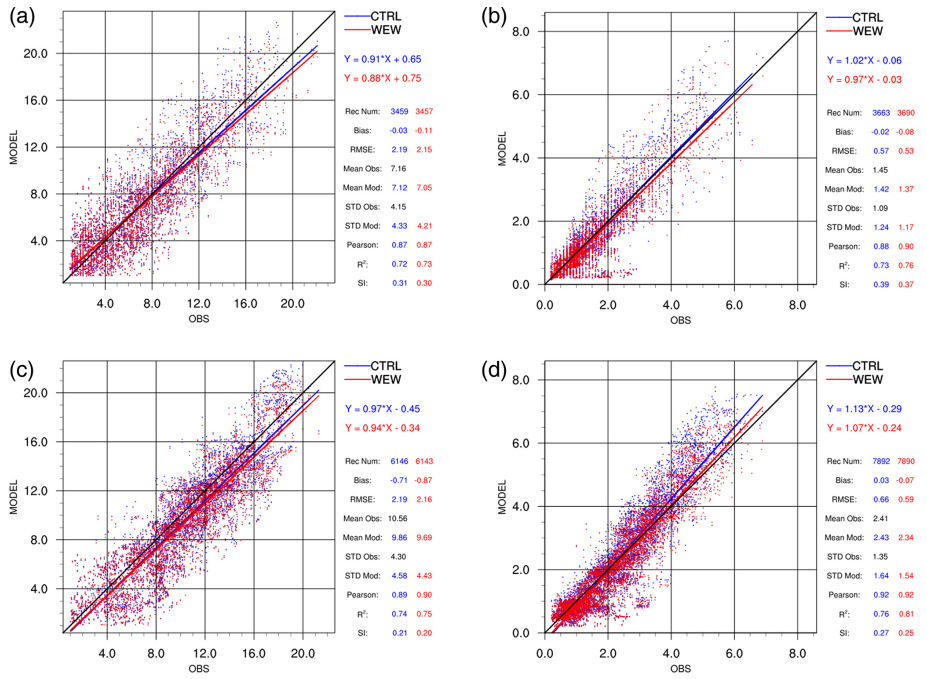


**Figure 12.** Scatter plots of the near surface wind speed exceeding 1 m s$^{-1}$ (**a** and **c**) and the significant wave height exceeding 0.2 m (**b** and **d**). *y* axis presents the model-estimated values and *x* axis the buoys observations (**a** and **b**) and the satellite estimations (**c** and **d**). CTRL and WEW evaluation results are shown in blue and red colors respectively.





GMDD
8, 4075–4112, 2015



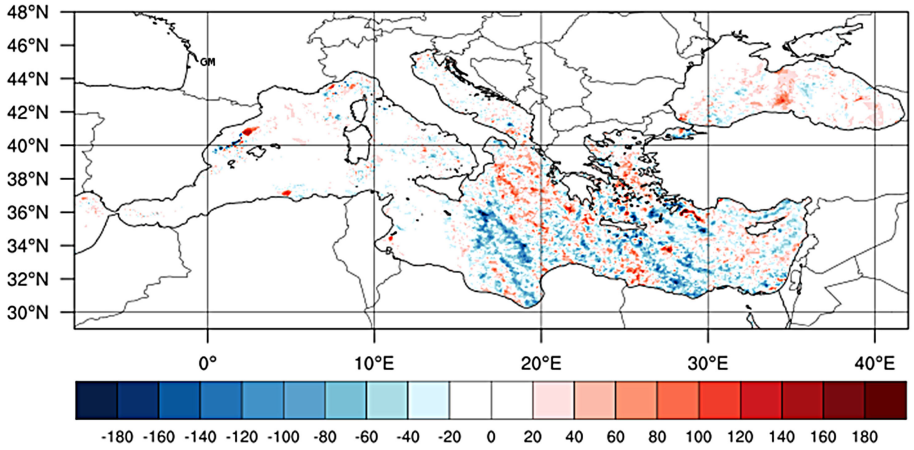


**Figure 13.** Spatial distribution of the averaged PBL height (in m) difference (WEW-CTRL).





GMDD
8, 4075–4112, 2015



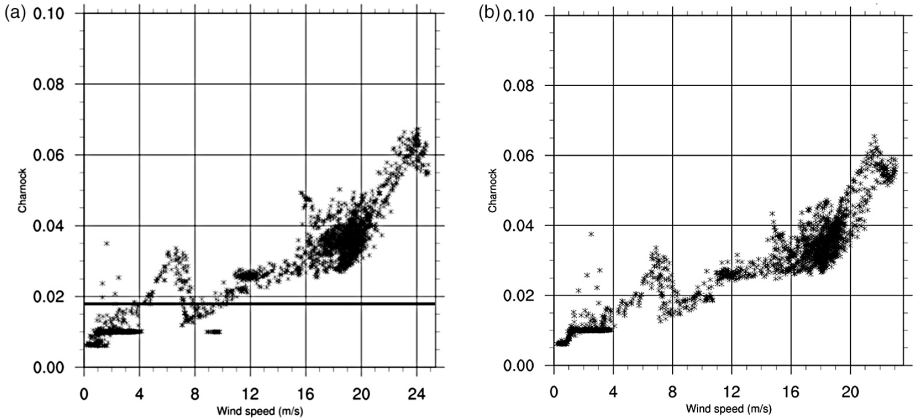


**Figure 14.** Charnock coefficient dependence to the wind speed in **(a)** offline coupled simulations. The thick solid line indicates the constant Charnock value (0.018) in the MYJ surface layer parameterization scheme. **(b)** WEW simulations.





GMDD
8, 4075–4112, 2015





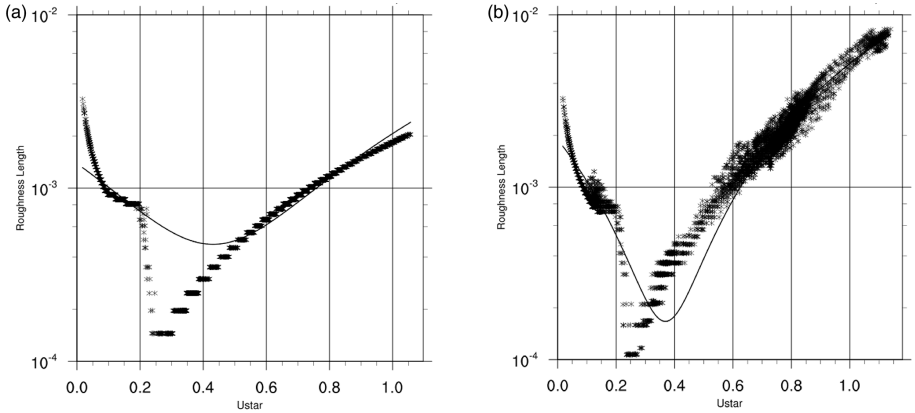


**Figure 15.** Roughness length (m) dependence to the friction velocity ($m\,s^{-1}$) for **(a)** the CTRL and **(b)** WEW experiments.





GMDD
8, 4075–4112, 2015